# Double-walled carbon nanotubes, a performing additive to enhance capacity retention of antimony anode in potassium-ion batteries

Vincent Gabaudan, Justine Touja, Didier Cot, Emmanuel Flahaut, Lorenzo Stievano, Laure Monconduit

▶ **To cite this version:**

Vincent Gabaudan, Justine Touja, Didier Cot, Emmanuel Flahaut, Lorenzo Stievano, et al.. Double-walled carbon nanotubes, a performing additive to enhance capacity retention of antimony anode in potassium-ion batteries. Electrochemistry Communications, 2019, 105, pp.106493. 10.1016/j.elecom.2019.106493 . hal-02196162

**HAL Id: hal-02196162**
**https://hal.science/hal-02196162**

Submitted on 26 Jul 2019

**HAL** is a multi-disciplinary open access archive for the deposit and dissemination of scientific research documents, whether they are published or not. The documents may come from teaching and research institutions in France or abroad, or from public or private research centers.

L'archive ouverte pluridisciplinaire **HAL**, est destinée au dépôt et à la diffusion de documents scientifiques de niveau recherche, publiés ou non, émanant des établissements d'enseignement et de recherche français ou étrangers, des laboratoires publics ou privés.

Electrochemistry Communications 105 (2019) 106493

Contents lists available at ScienceDirect

Electrochemistry Communications

journal homepage: www.elsevier.com/locate/elecom

Full communication

# Double-walled carbon nanotubes, a performing additive to enhance capacity retention of antimony anode in potassium-ion batteries

Vincent Gabaudan[a,b], Justine Touja[a,b], Didier Cot[c], Emmanuel Flahaut[d], Lorenzo Stievano[a,b], Laure Monconduit[a,b,*]

[a] ICGM, CNRS, Université de Montpellier, Montpellier, France
[b] Réseau sur le Stockage Électrochimique de l'Énergie (RS2E), CNRS, Amiens, France
[c] Institut Européen des Membranes, CNRS, Université de Montpellier, Montpellier, France
[d] CIRIMAT, CNRS, Université Toulouse III - Paul Sabatier, INPT, Toulouse, France

ARTICLE INFO

*Keywords:*
Potassium-ion batteries
Negative electrodes
Composites
Antimony
Carbon nanotubes

ABSTRACT

The effect of carbon additives on electrode formulation of bulk antimony was investigated in potassium-ion batteries. Several types of carbon including conventional carbon black, graphite and double-walled carbon nanotubes (DWCNT), employed as conductive agents, were found to play a non-negligible role on the electrochemical performance of antimony. While DWCNT alone show no reversible $K^+$ storage compared to the other carbons, the Sb/DWCNT electrode exhibits better capacity retention and rate capability than Sb formulated with usual carbon additives or even with graphite. This can be ascribed to the specific structure of DWCNT acting not only as conductive additive but also as a mechanical reinforcement for the whole electrode, which has to withstand the large volume change of antimony during potassiation/depotassiation cycles.

## 1. Introduction

Owing to their high energy density, Li-ion batteries (LIB) have been widely commercialized to power portables electronic devices and electric vehicles, and have been proposed as a system of choice for large scale energy storage [1]. However, the extensive use of Li for nomad applications coupled to its uneven distribution on Earth's crust may cause price volatility in the future, and hamper a wider application of LIB. For this reason, batteries operating with more abundant and low cost materials such as Na-ion batteries (NIB) and K-ion batteries (KIB) have recently emerged [2].

Even though the research devoted to KIB is still at an early stage, this technology appears as very promising given the low potential of the $K^+/K$ redox couple allowing the development of high energy density batteries. Regarding the negative electrode, most studies mainly focus on carbonaceous materials such as graphite, hard carbon, soft carbon or carbons nanotubes. These materials show interesting cycling performance but limited specific capacity compared to alloying materials which form binary compounds with potassium [3]. Among them, antimony, appears as a promising candidate owing to its relatively low operating voltage and its high specific capacity of 660 mAh/g corresponding to the formation of $K_3Sb$ [4,5]. One of the critical issues of Sb, however, is the huge volume expansion (~400%) occurring during the reversible potassiation/depotassiation process, which leads to electrode pulverization, extensive electrolyte degradation on the continuously formed fresh electrode surface and rapid capacity fading [6]. Several strategies have been proposed to overcome this drawback such as improving the electrolyte by using additives. However, the well-known fluoroethylene carbonate, extensively applied in LIB and NIB, appears to have no beneficial effect in KIB [7,8]. Embedding Sb nanoparticles in porous carbon matrixes notably improves the performance, but often involves trickier synthesis protocols and usually leads to poor coulombic efficiency (CE) due to the large surface of carbon exposed to the electrolyte degradation [5,9–11]. On the other hand, MXene materials are well known to offer fast diffusion kinetics owing two their two dimensional open framework showing interesting mechanical properties of flexibility and free standing. In that way, An et al. introduced Sb metal particles in MXene paper showing impressive capacity retention over 500 cycles [12].

Inspired by the research on LIB and NIB, an alternative approach to mitigate volume expansion in alloy materials is playing with binder and carbon additives in the electrode formulation [13]. This last approach is applied here, where double-walled carbon nanotubes (DWCNT) are used instead of other conventional carbon additives in the formulation

* Corresponding author at: ICGM, CNRS, Université de Montpellier, Montpellier, France.
*E-mail addresses:* vincent.gabaudan@etu.umontpellier.fr (V. Gabaudan), flahaut@chimie.ups-tlse.fr (E. Flahaut), lorenzo.stievano@umontpellier.fr (L. Stievano), laure.monconduit@umontpellier.fr (L. Monconduit).

https://doi.org/10.1016/j.elecom.2019.106493
Received 13 June 2019; Received in revised form 9 July 2019; Accepted 10 July 2019
Available online 12 July 2019
1388-2481/ © 2019 The Authors. Published by Elsevier B.V. This is an open access article under the CC BY-NC-ND license (http://creativecommons.org/licenses/BY-NC-ND/4.0/).

to improve the cycling performance of bulk Sb. Indeed, given their specific structure, DWCNT are expected to act not only as a conductive additive assuring the electrical percolation in the electrode, but also to reinforce its mechanical properties owing to their bundle network structure [14].

## 2. Materials and methods

Commercial antimony powder (325 mesh, 99.5%, Alfa Aesar) was mixed with different types of carbonaceous conductive additives and carboxymethyl cellulose binder (DS = 0.7, Mw = 250,000, Sigma Aldrich) in weight ratio 70/18/12, respectively. These proportions were chosen given the excellent performance obtained with them in LIB [15]. Four different carbon additives were investigated: a mixture of carbon black (C65, BET = 65 $m^2$/g, Timcal) and vapor ground carbon fibers (VGCF-S, BET = 15 $m^2$/g, Showa Denko) in weight ratio 50/50, Super P (BET = 62 $m^2$/g, Alfa Aesar), Graphite (SLP6, BET = 15.5 $m^2$/g, Timcal) and double-walled carbon nanotubes (DWCNT, BET = 958 $m^2$/g). The detailed synthesis of the DWCNT is described elsewhere [16]. In short, they were grown at 1000 °C by catalytic chemical vapor deposition of a mixture of methane and hydrogen on a Co:Mo MgO-based catalyst with additions of molybdenum oxide (elemental composition: $Mg_{0.99}Co_{0.0075}Mo_{0.0025}O$). The catalytic support was removed by processing the material with a concentrated HCl aqueous solution and further washing by deionised water. The inner and outer diameters ranged from 0.5 to 2.5 nm and from 1.2 to 3.2 nm, respectively. The median inner diameter was 1.3 nm and the median outer diameter was 2.0 nm. Deionised water was added to the different mixtures, which were then ball milled in a planetary mill for 1 h. The obtained slurries were tape casted onto copper foils (17.5 μm thick, 99.9%, Goodfellow), dried at room temperature for 24 h and subsequently at 80 °C overnight under dynamic vacuum. The loading of the obtained electrodes (antimony plus carbon) was 1.5–2 mg/$cm^2$. In order to study the specific influence of DWCNT on electrode formulation, two other Sb/DWCNT/CMC weight ratios were investigated: 63/25/12 and 78/10/12. Reference electrodes prepared with the four carbon additives only were also formulated with CMC binder in weight ratio 70/30. The electrolyte was prepared by dissolving 0.8 mol/L of potassium bis(fluorosulfonyl)imide (KFSI, 99.9% purity, Solvionic) into a 1:1 (v/v) mixture of ethylene carbonate (EC, anhydrous, 99% purity, Alfa Aesar) and diethyl carbonate (DEC, anhydrous, purity ≥99%, Sigma Aldrich). Coin cells were assembled in an Ar-filled glove box against K metal (Sigma Aldrich) as counter and reference electrode with a glass fiber separator (Whatman GF/D) soaked with the electrolyte. A polypropylene membrane (Celgard) was added between the electrode and the glass fiber separator for the coin cells cycled before the scanning electron microscopy (SEM) characterizations, performed with Hitachi S-4800 microscope. X-ray diffraction (XRD) patterns were collected on a Panalytical X'Pert diffractometer with the Cu Kα radiation. Raman spectra were measured on a LabRAM ARAMIS spectrometer equipped with CCD detector and 50× optical microscope objective using an excitation laser at 633 nm. The characterization of the commercial antimony powder is given in Fig. S1. The XRD pattern can be fully indexed with hexagonal antimony (ICSD code 064695). The SEM image of commercial powder shows a global repartition from 2 to 40 μm in the agreement with the supplier given size of 325 mesh. The four carbon additives were characterized by XRD, Raman spectroscopy and nitrogen adsorption/desorption, as shown in Fig. S2. Galvanostatic charge-discharge profiles were conducted on MPG2 potentiostat (Biologic) at a current rate of C/2 (i.e., 1 mol of K per mole of Sb in 2 h) between 0.0 and 2.0 V. All the capacities, reproducible for a minimum of two coin-cells, are reported in mAh per g of composite (notified Sb + C) taking into account that carbon additives participate to the measured capacity.

## 3. Results and discussion

Fig. 1 shows the galvanostatic charge/discharge profiles of Sb electrodes formulated with different carbon additives. The electrochemical signatures of the carbons alone are given in the insets and their characteristics and capacities are reported in the Table 1. Overall, all first cycle curves are rather similar and dominated by the reversible potassiation/depotassiation of Sb [4]. Regarding the signature of the different carbons, the potential of the first discharge of DWCNT electrode is particularly high at 1 V as previously shown by Zhao et al., [17] while that of the other materials is around 0.5–0.2 V. The large first discharge capacity of the DWCNT electrode is likely due to electrolyte decomposition, possibly enhanced by to the large surface area of DWCNT [18]. In this case, the lack of electrochemical reversible activity resembles that of multi-walled carbon nanotubes rather than that of single-walled ones, which instead reversibly store $K^+$ [17]. Moreover, potassium storage in DWCNT is not reversible, whereas the three other carbons show relatively stable potassium storage (insets Fig. 1 and Table 1). For all Sb/carbon electrodes, the specific first discharge capacity varies from 533 to 600 mAh/$g_{(Sb+C)}$. This value can be compared with their expected capacity (in red in Table 1) calculated taking into account the experimental capacity of the pure carbon electrodes and the theoretical capacity of Sb (660 mAh/g). Among Sb/Super P, Sb/C65/VGCF, Sb/graphite and Sb/DWCNT electrodes, the latter presents the best experimental first cycle CE of 88%, very close to 86%, the expected value calculated from the CE of the corresponding pure carbon electrode, whereas all the other carbons present lower experimental CE, which is even much lower than the expected values (> 95%) calculated as described above. This is rather surprising considering the limited reversibility of DWCNT vs. K compared to the other carbon electrodes, indicating that antimony clearly works better as an electrode material in the presence of DWCNT than formulated with the other tested carbons. The reversible capacity of the first cycle is around 470 mAh/$g_{(Sb+C)}$ independently of the carbon additive, corresponding to the insertion of $K^+$ in carbon and the partial alloying of K with Sb in all cases excepted for Sb/DWCNT where DWCNT show no reversible $K^+$ storage.

The cycling stability of the four electrodes at C/2 current rate (110 mA/g) is compared in Fig. 2a. Both Sb/DWCNT and Sb/C65/VGCF show stable capacity retention during the first cycles, whereas the capacity of Sb/Super P progressively decreases and that of Sb/Graphite undergoes rapid fading after 10 cycles. The low capacity retention of the latter can be explained by the large volume expansion (400% for Sb to $K_3Sb$ and 60% for $C_{gr}$ to $KC_8$) expected for this electrode as well as the combination of very distinct morphologies of Sb and $C_{gr}$ particles (Fig. 3), not adapted to long term cycling (vide infra). It is interesting to notice that the electrodes presenting the best capacity retention, namely Sb/DWCNT and Sb/C65/VGCF, are made of carbon fibers which enhance the mechanical strength and assure a good electric conductivity in the electrode [19]. In summary, Sb/DWCNT exhibits better capacity retention with 440 mAh/$g_{(Sb+C)}$ after 40 cycles when the capacity of the other electrodes have already faded.

Fig. 2b shows the rate capability of Sb/DWCNT and Sb/C65/VGCF, both electrodes showing stable capacity over at least 20 cycles (Fig. 2a). Sb/DWCNT exhibits high rate performance, delivering a stable capacity of 453 mAh/$g_{(Sb+C)}$ (close to the expected value of 462 mAh/g) at 4C (880 mA/g) whereas for the Sb/C65/VGCF electrode the capacity decreases from 344 mAh/$g_{(Sb+C)}$ to 280 mAh/$g_{(Sb+C)}$ over 5 cycles at the same rate. This result points out that the addition of DWCNT provides high electrode robustness even over fast potassiation/depotassiation.

As Sb/DWCNT exhibits the best cycle life, different DWCNT weight ratios were investigated in the Sb electrodes to check further possible improvements of the performance. Fig. 2c shows the first cycle with the corresponding CE of the different Sb/DWCNT electrodes. Considering the electrochemical activity of DWCNT only in the first discharge, Table 2 reports the experimental and the expected capacities measured

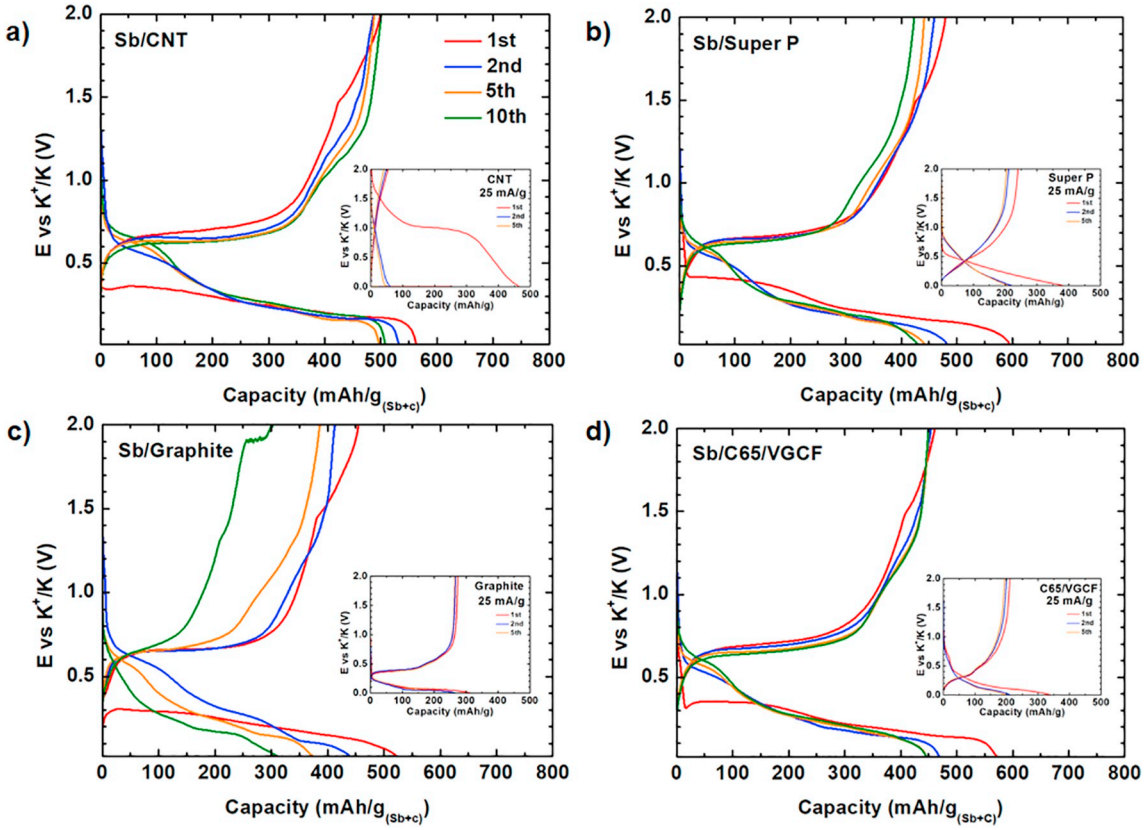


**Fig. 1.** Galvanostatic profiles of Sb formulated with four different carbon additives recorded at C/2 between 0 and 2 V versus K metal. The insets show the electrochemical signature of the carbon electrode without antimony at a current density of 25 mA/g. a) Sb/DWCNT, b) Sb/Super P, c) Sb/graphite, d) Sb/C65/VGCF.

for the three Sb/DWCNT electrodes. While the first cycle CE is very close to the expected one (88 vs 86%) for the 70/18 Sb/DWCNT ratio, the same value is not obtained for the other two formulations, less and more rich in Sb, confirming that the best capacity retention strongly depends on the optimization of the electrode formulation. In all cases, the CE reaches 99% after two cycles before rapidly decreasing, testifying the gradual electrolyte decomposition which also contributes to the gradual drop in capacity. In half-cell configuration, the high reactivity of metallic K counter electrode was already shown to induce a cross-talk mechanism between the electrodes, harmful for the electrolyte stability and thus for the battery cycle life [20]. Investigation in full cell against a real positive electrode is thus necessary to avoid this bias in the evaluation of the electrochemical performance. From this study, which will need to be further refined, the 70/18/12 ratio appears as the best compromise for the first cycle CE as well as for the cyclability. This is slightly different from Sb/$C_{gr}$ composites prepared by magneto ball milling with different weight ratios [8]. Increasing the amount of carbon graphite in the composite result in better cycle life and CE but lower overall capacities.

In order to investigate the capacity fading mechanism, SEM images

**Table 1**
Capacities of carbone and Sb/carbone electrodes observed in Fig. 1. The red values have been calculated taking into account the experimental capacity of carbon electrodes and the theoretical one of Sb i.e. (660 mA/g). The BET surfaces of the four different carbons are given for indication.

| | | Carbone electrodes | | Sb/Carbone electrodes | |
|---|---|---|---|---|---|
| | BET surface ($m^2$/g) | 1st Discharge/charge capacity (mAh/g) | Reversible capacity after 10 cycles (mAh/g) | 1st Discharge/charge capacity (mAh/g) | CE (%) |
| DWCNT | 958 | 465/54 | 35 | 542 (546)/479 (471) | 88.4 (86%)* |
| Super P | 62 | 385/240 | 205 | 600 (531)/480 (505) | 80 (95%)* |
| Graphite | 15.5 | 315/274 | 268 | 533 (519)/455 (511) | 85.4 (98%)* |
| C65/VGCF | 65/15 | 343/210 | 190 | 578 (523)/462 (500) | 79.9 (95.6%)* |

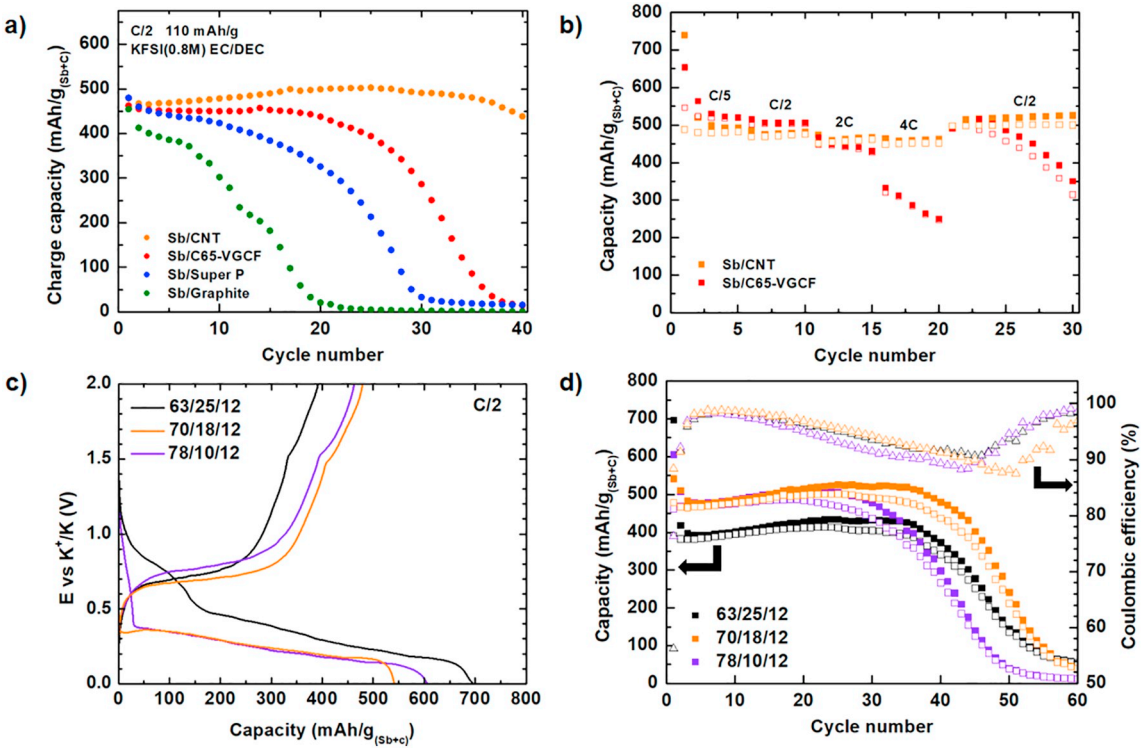


**Fig. 2.** a) Reversible capacity as a function of cycle number for the four Sb/C electrodes, b) Rate capability of Sb/DWCNT and Sb/C65/VGCF electrodes from C/5 to 4C rate, c) 1st cycle of Sb/DWCNT electrode with different weight ratios d) the corresponding capacity retention with CE.

of pristine electrodes were compared to those of electrodes after 30 cycles (Fig. 3). On the one hand, the pristine electrodes present Sb micro-particles uniformly dispersed on the electrode surface. Very distinct morphologies are observed for Sb/Graphite with the presence of graphitic flakes, and Sb/DWCNT which is rather compact, DWCNT and CMC creating a dense network around the Sb particles. On the other hand, Sb/C65/VGCF and Sb/Super P reveal a similar surface morphology appearing more porous than the other two materials. The very different electrode surfaces associated to the specific electrochemical signature of the four Sb/C composites prompted us to investigate the formation and the evolution of the SEI by X-ray photoelectron spectroscopy and impedance spectroscopy. The measurements are in progress and will be the core of a follow-up paper. After 30 cycles, the Sb/graphite electrode was totally detached from the current collector when the cells were opened whereas the three other electrodes were intact. The loss of electronic contact between electrode and current collector explains the rapid capacity fading of Sb/graphite. The Sb/DWCNT electrode shows a relatively homogeneous surface without cracks. The specific morphology of DWCNT allows keeping a good electronic percolation with Sb particles and current collector, accommodating the volume change over the potassiation/depotassiation process. The three other composites display Sb particles covered by

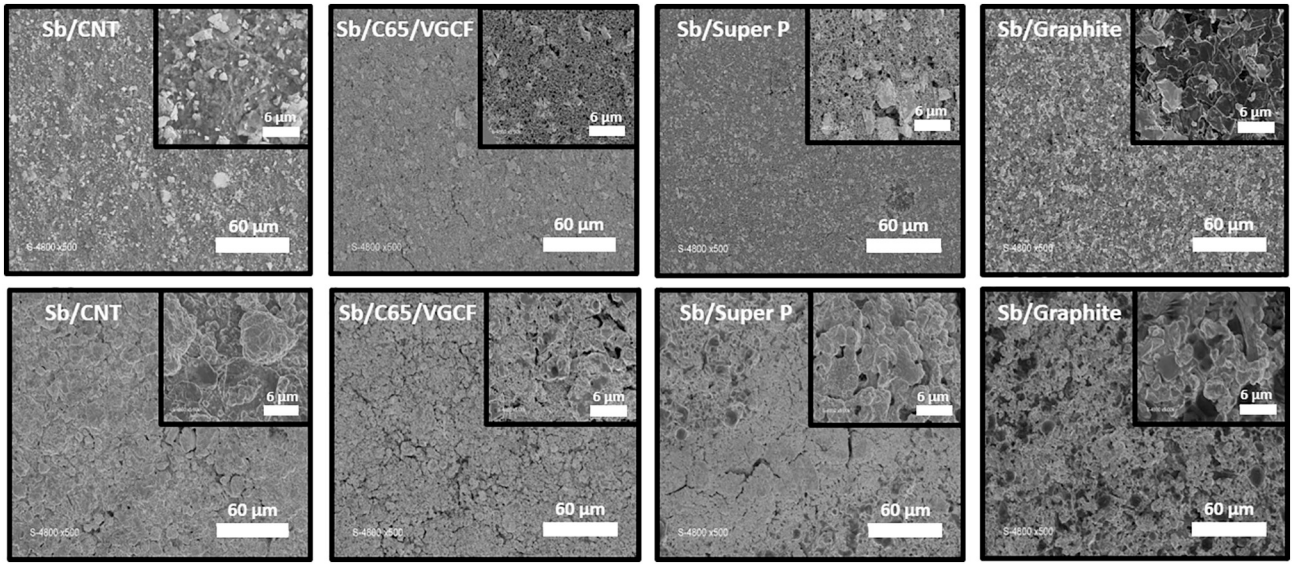


**Fig. 3.** SEM images of pristine electrodes top and electrodes after 30 cycles bottom. From the left to the right: Sb/DWCNT, Sb/C65/VGCF, Sb/Super P and Sb/graphite electrode respectively.

**Table 2**
Experimental and theoretical capacities of Sb/DWCNT electrodes observed in Fig. 2c and d. The red values have been calculated taking into account the experimental capacity of carbon electrodes and the theoretical one of Sb i.e. (660 mA/g).

| | 63/25 | 70/18 | 78/10 |
|---|---|---|---|
| Experimental 1st discharge | 695 | 542 | 610 |
| Theoretical 1st discharge | 532 (416+116,5) | 546 (462+84) | 561,5 (515+46,5) |
| Experimental 1st charge | 390 | 479 | 460 |
| Theoretical 1st charge | 429 (416+13) | 471 (462+9) | 520 (515+5) |
| CE (1st cycle) | 56.1 (80.6) | 88.4 (86.3) | 75.4 (92.6) |
| Charge capacity after 30 cycles | 405 | 491 | 437 |

a black coating surely due to electrolyte decomposition, which is enhanced in KIB compared to LIB and SIB. On the Sb/C65/VGCF electrode surface, some particles appear isolated while Sb/Super P electrode exhibits some cracks. The combination of the efficient reversible potassiation of Sb, with both a good electronic percolation and mechanical strength brought by DWCNT, seems to be a promising approach to improve the electrode performance of in KIB.

## 4. Conclusions

The influence of carbon additives on the cycling performance of bulk Sb in K-ion half-cells was investigated for the first time. This study underlines the crucial role of carbon additives in Sb-based composite electrodes for KIB, and these findings might be extended to other alloy materials. While DWCNT were not expected to provide a specific advantage due to their absence of reversible electrochemical activity vs. K, they nevertheless represent an excellent additive for Sb electrodes allowing a considerable extension of the lifespan of formulated electrodes. Indeed, the use of 18 wt% DWCNT as conductive additive in Sb electrodes formulated with CMC improved the capacity retention and the rate capabilities of bulk Sb electrodes. DWCNT appears to be much more efficient than other conventional carbon additives, such as C65/VGCF, super P and graphite, which react electrochemically with K and are not beneficial to the Sb composite electrode. On the other hand, DWCNT are more inert vs. K (at least after the first discharge) and act as an excellent additive with both good mechanical and electrical conductivity properties. Indeed, the specific structure of DWCNT greatly contributes to the stabilization of the electrode integrity over the potassiation/depotassiation process. These results confirm that the addition of DWCNT to the formulation is an interesting strategy for the improvement of the performance of alloying electrode materials for KIB. The intrinsic nature of DWCNT seems to play a key role in the electrochemical behaviour of the studied composites [17]. Nitrogen-doped DWCNT, reported to improve the adsorption of $K^+$ on surface defects and edges, could also be an interesting additive for negative electrodes in KIB and will be the object of a future study [21,22]. In parallel, a serious evaluation of electrolyte reactivity as a function of the type of carbon, either used as active material or as additive in electrodes for KIB, has to be forecasted.

## Acknowledgements

The authors thank the French National Research Agency for the financial support (STORE-EX Labex Project ANR-10-LABX-76-01). Authors thank also CNRS, Projets exploratoires (PEPS) for their financial support.

## Appendix A. Supplementary data

Supplementary data to this article can be found online at https://doi.org/10.1016/j.elecom.2019.106493.

## References

[1] B. Dunn, H. Kamath, J.-M. Tarascon, Electrical energy storage for the grid: a battery of choices, Science 334 (2011) 928–935, https://doi.org/10.1126/science.1212741.
[2] K. Kubota, M. Dahbi, T. Hosaka, S. Kumakura, S. Komaba, Towards K-ion and Na-ion batteries as “beyond Li-ion”, Chem. Rec. 18 (2018) 459–479, https://doi.org/10.1002/tcr.201700057.
[3] I. Sultana, M.M. Rahman, Y. Chen, A.M. Glushenkov, Potassium-ion battery anode materials operating through the alloying-dealloying reaction mechanism, Adv. Funct. Mater. 28 (2018) 1703857, , https://doi.org/10.1002/adfm.201703857.
[4] W.D. McCulloch, X. Ren, M. Yu, Z. Huang, Y. Wu, Potassium-ion oxygen battery based on a high capacity antimony anode, ACS Appl. Mater. Interfaces 7 (2015) 26158–26166, https://doi.org/10.1021/acsami.5b08037.
[5] Z. Yi, N. Lin, W. Zhang, W. Wang, Y. Zhu, Y. Qian, Preparation of Sb nanoparticles in molten salt and their potassium storage performance and mechanism, Nanoscale 10 (2018) 13236–13241, https://doi.org/10.1039/C8NR03829E.
[6] V. Gabaudan, R. Berthelot, L. Stievano, L. Monconduit, Inside the alloy mechanism of Sb and Bi electrodes for K-ion batteries, J. Phys. Chem. C 122 (2018) 18266–18273, https://doi.org/10.1021/acs.jpcc.8b04575.
[7] W. Zhang, W.K. Pang, V. Sencadas, Z. Guo, Understanding high-energy-density Sn4P3 anodes for potassium-ion batteries, Joule 2 (2018) 1534–1547, https://doi.org/10.1016/j.joule.2018.04.022.
[8] I. Sultana, M.M. Rahman, J. Liu, N. Sharma, A.V. Ellis, Y. Chen, A.M. Glushenkov, Antimony-carbon nanocomposites for potassium-ion batteries: insight into the failure mechanism in electrodes and possible avenues to improve cyclic stability, J. Power Sources 413 (2019) 476–484, https://doi.org/10.1016/j.jpowsour.2018.12.017.
[9] Y. An, Y. Tian, L. Ci, S. Xiong, J. Feng, Y. Qian, Micron-sized nanoporous antimony with tunable porosity for high-performance potassium-ion batteries, ACS Nano 12 (2018) 12932–12940, https://doi.org/10.1021/acsnano.8b08740.
[10] H. Wang, X. Wu, X. Qi, W. Zhao, Z. Ju, Sb nanoparticles encapsulated in 3D porous carbon as anode material for lithium-ion and potassium-ion batteries, Mater. Res. Bull. 103 (2018) 32–37, https://doi.org/10.1016/j.materresbull.2018.03.018.
[11] J. Zheng, Y. Yang, X. Fan, G. Ji, X. Ji, H. Wang, S. Hou, M.R. Zachariah, C. Wang, Extremely stable antimony–carbon composite anodes for potassium-ion batteries, Energy Environ. Sci. 12 (2019) 615–623, https://doi.org/10.1039/C8EE02836B.
[12] Y. Tian, Y. An, S. Xiong, J. Feng, Y. Qian, A general method for constructing robust, flexible and freestanding MXene@metal anodes for high-performance potassium-ion batteries, J. Mater. Chem. A 7 (2019) 9716–9725, https://doi.org/10.1039/C9TA02233C.
[13] V. Sivasankaran, C. Marino, M. Chamas, P. Soudan, D. Guyomard, J.C. Jumas, P.E. Lippens, L. Monconduit, B. Lestriez, Improvement of intermetallics electrochemical behavior by playing with the composite electrode formulation, J. Mater. Chem. 21 (2011) 5076, https://doi.org/10.1039/c0jm03831h.
[14] B.J. Landi, M.J. Ganter, C.D. Cress, R. DiLeo, R.P. Raffaelle, Carbon nanotubes for lithium ion batteries, Energy Environ. Sci. 2 (2009) 638–654, https://doi.org/10.1039/b904116h.
[15] V. Sivasankaran, C. Marino, M. Chamas, P. Soudan, D. Guyomard, J.-C. Jumas, P.-E. Lippens, L. Monconduit, B. Lestriez, Improvement of intermetallics electrochemical behavior by playing with the composite electrode formulation, J. Mater. Chem. 21 (2011) 5076–5082.
[16] E. Flahaut, R. Bacsa, A. Peigney, C. Laurent, Gram-scale CCVD synthesis of double-walled carbon nanotubes, Chem. Commun. (2003) 1442, https://doi.org/10.1039/

b301514a.
[17] X. Zhao, Y. Tang, C. Ni, J. Wang, A. Star, Y. Xu, Free-standing nitrogen-doped cup-stacked carbon nanotube mats for potassium-ion battery anodes, ACS Appl. Energy Mater. 1 (2018) 1703–1707, https://doi.org/10.1021/acsaem.8b00182.
[18] S.Y. Chew, S.H. Ng, J. Wang, P. Novák, F. Krumeich, S.L. Chou, J. Chen, H.K. Liu, Flexible free-standing carbon nanotube films for model lithium-ion batteries, Carbon 47 (2009) 2976–2983, https://doi.org/10.1016/j.carbon.2009.06.045.
[19] M. Endo, Y. Kim, T. Hayashi, K. Nishimura, T. Matusita, K. Miyashita, M. Dresselhaus, Vapor-grown carbon fibers (VGCFs), Carbon 39 (2001) 1287–1297, https://doi.org/10.1016/S0008-6223(00)00295-5.
[20] L. Madec, V. Gabaudan, G. Gachot, L. Stievano, L. Monconduit, H. Martinez, Paving the way for K-ion batteries: role of electrolyte reactivity through the example of Sb-based electrodes, ACS Appl. Mater. Interfaces 10 (2018) 34116–34122, https://doi.org/10.1021/acsami.8b08902.
[21] Y. Xu, C. Zhang, M. Zhou, Q. Fu, C. Zhao, M. Wu, Y. Lei, Highly nitrogen doped carbon nanofibers with superior rate capability and cyclability for potassium ion batteries, Nat. Commun. 9 (2018) 1720, , https://doi.org/10.1038/s41467-018-04190-z.
[22] P. Xiong, X. Zhao, Y. Xu, Nitrogen-doped carbon nanotubes derived from metal-organic frameworks for potassium-ion battery anodes, ChemSusChem 11 (2018) 202–208, https://doi.org/10.1002/cssc.201701759.